Substructuring with Nonlinear Reduced Order Models and Interface Reduction with Characteristic Constraint Modes

Robert J. Kuether[1]
Matthew S. Allen[2]
Department of Engineering Physics, University of Wisconsin-Madison, Madison, Wisconsin, 53706, USA

Substructuring methods have been widely used in structural dynamics to divide large, complicated finite element models into smaller substructures. For linear systems, many methods have been developed to reduce the subcomponents down to a low order set of equations using a special set of component modes, and these are then assembled to approximate the dynamics of a large scale model. In this paper, a substructuring approach is developed for coupling geometrically nonlinear structures, where each subcomponent is drastically reduced to a low order set of nonlinear equations using a truncated set of fixed-interface and characteristic constraint modes. A non-intrusive method to fit the nonlinear reduced order model (NLROM) is used to identify the low order equations directly from a finite element model built within a commercial software package. The NLROMs are then assembled to approximate the nonlinear differential equations of the global assembly. The method is demonstrated on the coupling of two geometrically nonlinear plates with simple supports at all edges. The plates are joined at a continuous interface through the rotational degrees-of-freedom (DOF), and the nonlinear normal modes (NNMs) of the assembled equations are computed to validate the equations. The proposed substructuring approach reduces a 12,861 DOF nonlinear finite element model down to only 22 DOF, while maintaining the accuracy to compute the first three NNMs of the full order model.

I. Introduction

COMPONENT mode synthesis methods divide a structure into a set of smaller subcomponents, reduce these models down to a low order set of equations, and assemble them to approximate the dynamics of the global assembly. In finite element analysis (FEA), a subcomponent is reduced with a small set of basis vectors, or component modes, offering equations of motion with significantly fewer degrees-of-freedom (DOF) compared to the full order subcomponent model. One popular substructuring approach, called the Craig-Bampton (CB) method, reduces each subcomponent with a truncated set of fixed-interface normal modes, and static constraint modes. Hurty first introduced this method for linear systems in [1], but Craig and Bampton later simplified it in [2]. When generating the CB models of subcomponents with a continuous interface (e.g. having many connecting DOF), the reduced order model (ROM) may still be prohibitively large since there is one constraint mode for each interface DOF. Castanier et al. [3] developed a ROM that takes the assembled CB ROMs, and performs a second modal analysis on the coupled mass and stiffness matrices corresponding to the interface DOF. This second modal analysis allows the constraint modes to be truncated into a small set of characteristic constraint (CC) modes, which capture the "characteristic" deformation at the interface. As a result, each subcomponent model uses a small number of basis vectors, making this an efficient approach for realistic structures having many DOF at the interface.

All prior works that have used the Craig-Bampton approach with characteristic constraint modes have been limited to linear subcomponents (although possibly joined by nonlinear springs). This work uses this basis to couple two geometrically nonlinear finite element models along a continuous interface. A nonlinear reduced order model (NLROM) is generated from an FEA model, which is built directly within a commercial FEA package, using a truncated set of fixed-interface and characteristic constraint modes as a basis, and then two nonlinear substructures are assembled to provide a low order set of nonlinear equations approximating the global assembly.

[1] Graduate Student, 534 Engineering Research Building, 1500 Engineering Drive, Madison, WI 53706-1609, rkuether@wisc.edu, AIAA Member.
[2] Associate Professor, 535 Engineering Research Building, 1500 Engineering Drive, Madison, WI 53706-1609, msallen@engr.wisc.edu, AIAA Lifetime Member.

Over the last decade or so, a variety of methods have been developed to generate ROMs of geometrically nonlinear finite element models, as reviewed in [4, 5]. These methods use a truncated set of linear eigenvectors to reduce the full order FEA model down to a set of low order, nonlinear modal equations. With this reduction, numerical integration of the system becomes significantly less expensive than direct integration of the full finite element model, and a closed form set of equations becomes available for other analysis (e.g. harmonic balance). This is helpful, because commercial software typically does not provide the equations of motion of a geometrically nonlinear system in closed form. Using the usual approach, the reduced order equations still have diagonal mass, damping and stiffness matrices, but these linear matrices are augmented by assuming that the geometric nonlinearity can be well approximated using quadratic and cubic polynomials in the modal coordinates. In order to determine the coefficients of these polynomials, a series of static load cases (either applied forces or enforced displacements) are used and a least squares problem is solved to obtain the polynomial coefficients.

Until recently, all of the works on this type of reduced order modeling sought to find a reduced order model for the entire structure of interest. While this can be very effective, it becomes exceedingly expensive if the system has too many modal degrees of freedom. Larger FEA models with a large modal density require many modes to capture the kinematics of the structure, in turn requiring a large number of static load cases to fit the nonlinear stiffness coefficients. For example, to find the polynomial coefficients for a 20-mode model one must apply 9,920 permutations of static loads, whereas a 50-mode model would require 161,800 [6]. This can be addressed to some extent using the procedure in [7], which uses the tangent stiffness matrix to more efficiently compute the polynomial coefficients. They demonstrated the procedure by reducing a 96,000 DOF model of a 9-bay panel to an 82 mode model, but even then it was challenging to determine which modes to include and what displacements to apply to determine the polynomial coefficients. This work proposes a substructuring concept that can be used to divide a complicated model into smaller components, each of which is far simpler and hence it is easier to create a validated model of the component. The subcomponent models can then be assembled to generate a NLROM of the assembly. One additional benefit, is that during the design stage the subcomponents are typically redesigned by different teams and independently of the global structure, and so it is more convenient to modify and recompute the models for smaller, simpler subcomponents rather than a larger, global model.

In [8], the authors originally proposed substructuring using a set of NLROMs that were generated with a set of free-interface modes, but it was found that far too many modes were required to obtain acceptable accuracy. A later publication [9] explored the use of fixed-interface and constraint modes (e.g. a Craig-Bampton ROM) on an assembly of two geometrically nonlinear beams, where the connecting interface had only 1-DOF. The new reduction basis improved the accuracy of the coupled equations significantly, as expected since in linear substructuring the Craig-Bampton basis has long been known to be far more efficient than a free-interface mode basis when the subcomponents are rigidly connected to each other. However, for an interface with more than a few DOF, the CB approach would be prohibitive since the number of constraint modes would be larger than what can be currently computed with the indirect NLROM approach. In this paper, characteristic constraint modes [3] will be used to decrease the number of static load cases required to fit the nonlinear coefficients in the polynomial form of the geometric nonlinearity, and the assembly of highly efficient NLROMs will provide an accurate approximation of a global assembly.

The paper is outlined as follows. Section II presents the theory behind Craig-Bampton nonlinear reduced order models with characteristic constraint modes (abbreviated as CC-NLROMs). The novel approach is then demonstrated in Section III on an example problem where two geometrically nonlinear flat plates with simple supports at the boundary are coupled at a continuous interface through the rotational degrees-of-freedom. The nonlinear normal modes of the assembly are then used to evaluate the accuracy of the nonlinear substructuring approach. The conclusions are presented in Section IV.

II. Theory

The discretized system of equations for an *N*-DOF, nonlinear finite element model can be written as

$$\mathbf{M}\ddot{\mathbf{x}} + \mathbf{K}\mathbf{x} + \mathbf{f}_{NL}(\mathbf{x}) = \mathbf{f}(t) \tag{1}$$

where $\mathbf{M}$ and $\mathbf{K}$ are the $N \times N$ linear mass and stiffness matrices, respectively, and $\mathbf{f}_{NL}(\mathbf{x})$ is the $N \times 1$ nonlinear restoring force vector describing the geometric nonlinearity. The $N \times 1$ vectors $\mathbf{x}$, $\dot{\mathbf{x}}$, and $\ddot{\mathbf{x}}$ are the displacement, velocity and acceleration, respectively. Each DOF in $\mathbf{x}$ can be partitioned into either boundary DOF ($\mathbf{x}_b$), or interior DOF ($\mathbf{x}_i$). The boundary DOF are either shared by an adjacent structure, or have an external load

$\mathbf{f}(t)$ applied to that location. The interior DOF are all the remaining coordinates of the system. The partitioned equations of motion become

$$\begin{bmatrix} \mathbf{M}_{ii} & \mathbf{M}_{ib} \\ \mathbf{M}_{bi} & \mathbf{M}_{bb} \end{bmatrix} \begin{Bmatrix} \ddot{\mathbf{x}}_i \\ \ddot{\mathbf{x}}_b \end{Bmatrix} + \begin{bmatrix} \mathbf{K}_{ii} & \mathbf{K}_{ib} \\ \mathbf{K}_{bi} & \mathbf{K}_{bb} \end{bmatrix} \begin{Bmatrix} \mathbf{x}_i \\ \mathbf{x}_b \end{Bmatrix} + \begin{Bmatrix} \mathbf{f}_{NL,i}(\mathbf{x}) \\ \mathbf{f}_{NL,b}(\mathbf{x}) \end{Bmatrix} = \begin{Bmatrix} \mathbf{0} \\ \mathbf{f}(t) \end{Bmatrix} \tag{2}$$

Following the derivation in [3], the fixed-interface modes and characteristic constraint modes can be generated from the system in Eq. (2). The fixed-interface modes are first calculated by fixing all boundary DOF and then performing a linear modal analysis with the linear mass and stiffness matrices $\mathbf{M}_{ii}$ and $\mathbf{K}_{ii}$. In the classical CB method [2], a set of static vectors, termed constraint modes, augment the fixed-interface modes to account for deformation at the interface. A constraint mode is computed for each boundary DOF by computing the static deflection to a unit displacement at the boundary DOF. The linear portion of the equations of motion in Eq. (2) are reduced with the CB transformation matrix

$$\begin{Bmatrix} \mathbf{x}_i \\ \mathbf{x}_b \end{Bmatrix} = \begin{bmatrix} \mathbf{\Phi}_{ik} & \mathbf{\Psi}_{ib} \\ \mathbf{0} & \mathbf{I} \end{bmatrix} \begin{Bmatrix} \mathbf{q}_k \\ \mathbf{x}_b \end{Bmatrix} = \mathbf{T}^{CB} \mathbf{q}^{CB} \tag{3}$$

where $\mathbf{\Phi}_{ik}$ is the $N_i \times N_k$ matrix of truncated fixed-interface modes, with each column being mass normalized, and $\mathbf{\Psi}_{ib}$ is the $N_i \times N_b$ matrix of constraint modes. Substituting Eq. (3) into Eq. (2) and pre-multiplying by the transpose $(\ )^{\mathrm{T}}$ of $\mathbf{T}^{CB}$, the linear portion of the reduced equations of motion become,

$$\begin{bmatrix} \mathbf{I} & \hat{\mathbf{M}}_{kb} \\ \hat{\mathbf{M}}_{bk} & \hat{\mathbf{M}}_{bb} \end{bmatrix} \begin{Bmatrix} \ddot{\mathbf{q}}_k \\ \ddot{\mathbf{x}}_b \end{Bmatrix} + \begin{bmatrix} \mathbf{\Lambda} & \mathbf{0} \\ \mathbf{0} & \hat{\mathbf{K}}_{bb} \end{bmatrix} \begin{Bmatrix} \mathbf{q}_k \\ \mathbf{x}_b \end{Bmatrix} = \begin{Bmatrix} 0 \\ \mathbf{f}(t) + \mathbf{r}(t) \end{Bmatrix} \tag{4}$$

The vector $\mathbf{r}(t)$ is the unknown equal and opposite reaction force that will be applied by the connecting structure, $\mathbf{I}$ is the identity matrix, and $\mathbf{\Lambda}$ is a diagonal matrix of squared natural frequencies for the fixed-interface modes. For FEA models with a very detailed mesh at the interface, there may be far too many constraint modes, $\mathbf{\Psi}_{ib}$, in the reduced basis. The method in [3] reduces the number of constraint modes to capture the deformation at the interface by first assembling the reduced, linear CB models with all of the interface DOF as,

$$\begin{bmatrix} \mathbf{I}^A_{k_A k_A} & \mathbf{0} & \hat{\mathbf{M}}^A_{k_A b} \\ \mathbf{0} & \mathbf{I}^B_{k_B k_B} & \hat{\mathbf{M}}^B_{k_B b} \\ \hat{\mathbf{M}}^A_{b k_A} & \hat{\mathbf{M}}^B_{b k_B} & \hat{\mathbf{M}}^A_{bb} + \hat{\mathbf{M}}^B_{bb} \end{bmatrix} \begin{Bmatrix} \ddot{\mathbf{q}}^A_{k_A} \\ \ddot{\mathbf{q}}^B_{k_B} \\ \ddot{\mathbf{x}}_b \end{Bmatrix} + \begin{bmatrix} \mathbf{\Lambda}^A_{k_A k_A} & \mathbf{0} & \mathbf{0} \\ \mathbf{0} & \mathbf{\Lambda}^B_{k_B k_B} & \mathbf{0} \\ \mathbf{0} & \mathbf{0} & \hat{\mathbf{K}}^A_{bb} + \hat{\mathbf{K}}^B_{bb} \end{bmatrix} \begin{Bmatrix} \mathbf{q}^A_{k_A} \\ \mathbf{q}^B_{k_B} \\ \mathbf{x}_b \end{Bmatrix} = \begin{Bmatrix} \mathbf{0} \\ \mathbf{0} \\ \mathbf{f}(t) \end{Bmatrix} \tag{5}$$

Performing a second modal analysis facilitates the reduction at the boundary DOF to a small number of characteristic constraint modes. An eigenvalue problem is performed on the linear mass and stiffness matrices of the interface in Eq. (5) as

$$\left[\left[\hat{\mathbf{K}}^A_{bb} + \hat{\mathbf{K}}^B_{bb}\right] - \omega^2 \left[\hat{\mathbf{M}}^A_{bb} + \hat{\mathbf{M}}^B_{bb}\right]\right] \boldsymbol{\psi}^{CC} = \mathbf{0} \tag{6}$$

The modes, $\boldsymbol{\psi}^{CC}$, are then truncated to form the $N_b \times N_c$ matrix $\mathbf{\Psi}^{CC}$. Using this basis, the new transformation matrix for the linear subcomponent in Eq. (2) becomes

$$\mathbf{x} = \begin{Bmatrix} \mathbf{x}_i \\ \mathbf{x}_b \end{Bmatrix} = \begin{bmatrix} \boldsymbol{\Phi}_{ik} & \boldsymbol{\Psi}_{ib} \\ \mathbf{0} & \mathbf{I} \end{bmatrix} \begin{bmatrix} \mathbf{I} & \mathbf{0} \\ \mathbf{0} & \boldsymbol{\Psi}^{CC} \end{bmatrix} \begin{Bmatrix} \mathbf{q}_k \\ \mathbf{q}_c \end{Bmatrix} = \begin{bmatrix} \boldsymbol{\Phi}_{ik} & \hat{\boldsymbol{\Psi}}_{ic} \\ \mathbf{0} & \hat{\boldsymbol{\Psi}}_{bc} \end{bmatrix} = \mathbf{T}^{CC}\mathbf{q} \tag{7}$$

$\hat{\boldsymbol{\Psi}}$ is now the $N \times N_c$ matrix of characteristic constraint modes which capture the motion of the interface for a single subcomponent. The total number of generalized coordinates for this reduction will be denoted as $m = N_k + N_\mathbf{c}$. The generalized $m \times 1$ vector $\mathbf{q}$ has significantly fewer DOF than the full order model in Eq. (1).

Substituting Eq. (7) into Eq. (2), and pre-multiplying by the transpose $(\ )^{\mathrm{T}}$ of the matrix $\mathbf{T}^{CC}$, the CC-NLROM becomes

$$\hat{\mathbf{M}}_{CC}\ddot{\mathbf{q}} + \hat{\mathbf{K}}_{CC}\mathbf{q} + \mathbf{T}^{CC\,\mathrm{T}} \begin{Bmatrix} \mathbf{f}_{NL,i}(\mathbf{q}) \\ \mathbf{f}_{NL,b}(\mathbf{q}) \end{Bmatrix} = \mathbf{T}^{CC\,\mathrm{T}} \begin{Bmatrix} \mathbf{0} \\ \mathbf{f}(t) + \mathbf{r}(t) \end{Bmatrix} \tag{8}$$

For the reduced model, the unknown nonlinear modal restoring force can be defined generally as

$$\mathbf{T}^{CC\,\mathrm{T}} \begin{Bmatrix} \mathbf{f}_{NL,i}(\mathbf{q}) \\ \mathbf{f}_{NL,b}(\mathbf{q}) \end{Bmatrix} = \boldsymbol{\theta}(q_1, q_2, \ldots, q_m) \tag{9}$$

The nonlinear function $\boldsymbol{\theta}(q_1, q_2, \ldots, q_m)$ depends on the modes used in the basis, and the form of nonlinearity in the physical model. Prior works with geometrically nonlinear structures [4, 5] assume that the nonlinear restoring force vector is well approximated as a quadratic and cubic polynomial function. The r^{th} row of this polynomial function is given as

$$\theta_r(q_1, q_2, \ldots, q_m) \approx \sum_{i=1}^{m}\sum_{j=i}^{m} B_r(i,j) q_i q_j + \sum_{i=1}^{m}\sum_{j=i}^{m}\sum_{k=j}^{m} A_r(i,j,k) q_i q_j q_k \tag{10}$$

The nonlinear stiffness coefficients A_r and B_r are not explicitly available for FEA models built directly in a commercial finite element package, so an indirect approach is used to find these values. Following the strategy of the Implicit Condensation method in [10], the coefficients are estimated by applying a series of static loads to the structure proportional to the shapes of the fixed-interface and characteristic constraint modes. Details on the load cases and the fitting procedure can be found in [6].

To facilitate the substructuring process, after fitting the nonlinear stiffness coefficients, the equations of motion are cast into a matrix form as done in [8, 9]. The subcomponent CC-NLROMs then can be coupled to any adjacent nonlinear (or linear) structure(s). For example, the unconstrained equations of motion for the assembly of two geometrically nonlinear subcomponents can be written as

$$\begin{bmatrix} \hat{\mathbf{M}}_{CC}{}^{A} & \mathbf{0} \\ \mathbf{0} & \hat{\mathbf{M}}_{CC}{}^{B} \end{bmatrix} \begin{Bmatrix} \ddot{\mathbf{q}}^{A} \\ \ddot{\mathbf{q}}^{B} \end{Bmatrix} + \begin{bmatrix} \hat{\mathbf{K}}_{CC}{}^{A} & \mathbf{0} \\ \mathbf{0} & \hat{\mathbf{K}}_{CC}{}^{B} \end{bmatrix} \begin{Bmatrix} \mathbf{q}^{A} \\ \mathbf{q}^{B} \end{Bmatrix} + \frac{1}{2} \begin{bmatrix} \mathbf{N}_1^{A}(\mathbf{q}^{A}) & \mathbf{0} \\ \mathbf{0} & \mathbf{N}_1^{B}(\mathbf{q}^{B}) \end{bmatrix} \begin{Bmatrix} \mathbf{q}^{A} \\ \mathbf{q}^{B} \end{Bmatrix}$$
$$+ \frac{1}{3} \begin{bmatrix} \mathbf{N}_2^{A}(\mathbf{q}^{A}) & \mathbf{0} \\ \mathbf{0} & \mathbf{N}_2^{B}(\mathbf{q}^{B}) \end{bmatrix} \begin{Bmatrix} \mathbf{q}^{A} \\ \mathbf{q}^{B} \end{Bmatrix} = \begin{matrix} \mathbf{T}^{CC,A\,\mathrm{T}} \begin{Bmatrix} \mathbf{0} \\ \mathbf{f}(t)^{A} + \mathbf{r}(t)^{A} \end{Bmatrix} \\ \mathbf{T}^{CC,B\,\mathrm{T}} \begin{Bmatrix} \mathbf{0} \\ \mathbf{f}(t)^{B} + \mathbf{r}(t)^{B} \end{Bmatrix} \end{matrix} \tag{11}$$

The matrices $\mathbf{N}_1(\mathbf{q})$ and $\mathbf{N}_2(\mathbf{q})$ are the quadratic and cubic nonlinear stiffness matrices, respectively, for each subcomponent model.

Compatibility requires that the generalized coordinates of each characteristic constraint mode must be equal, such that $\mathbf{q}_c^A = \mathbf{q}_c^B = \mathbf{q}_c$. This constraint equation plus the equations of motion in Eq. (11) fully characterize the system. However, the DOF, $\mathbf{q}^A$ and $\mathbf{q}^B$, must satisfy the constraints and hence they are not completely free, making the equations inconvenient to deal with. This is addressed by defining the substructure coupling matrix $\mathbf{L}$ and then using it to eliminate the redundant boundary DOF in Eq. (11), giving a transformation to a set of unconstrained coordinates

$$\begin{Bmatrix} \mathbf{q}_k^A \\ \mathbf{q}_c^A \\ \mathbf{q}_k^B \\ \mathbf{q}_c^B \end{Bmatrix} = \begin{bmatrix} \mathbf{I} & \mathbf{0} & \mathbf{0} \\ \mathbf{0} & \mathbf{0} & \mathbf{I} \\ \mathbf{0} & \mathbf{I} & \mathbf{0} \\ \mathbf{0} & \mathbf{0} & \mathbf{I} \end{bmatrix} \begin{Bmatrix} \mathbf{q}_k^A \\ \mathbf{q}_k^B \\ \mathbf{q}_c \end{Bmatrix} = \mathbf{L}\mathbf{q}_u \tag{12}$$

Substituting Eq. (12) into Eq. (11) and pre-multiplying by $\mathbf{L}^{\mathrm{T}}$, the equations of motion for the assembly become

$$\begin{aligned} &\mathbf{L}^{\mathrm{T}} \begin{bmatrix} \hat{\mathbf{M}}_{CC}{}^{A} & \mathbf{0} \\ \mathbf{0} & \hat{\mathbf{M}}_{CC}{}^{B} \end{bmatrix} \mathbf{L}\ddot{\mathbf{q}}_u + \mathbf{L}^{\mathrm{T}} \begin{bmatrix} \hat{\mathbf{K}}_{CC}{}^{A} & \mathbf{0} \\ \mathbf{0} & \hat{\mathbf{K}}_{CC}{}^{B} \end{bmatrix} \mathbf{L}\mathbf{q}_u + \frac{1}{2}\mathbf{L}^{\mathrm{T}} \begin{bmatrix} \mathbf{N}_1^A(\mathbf{q}^A) & \mathbf{0} \\ \mathbf{0} & \mathbf{N}_1^B(\mathbf{q}^B) \end{bmatrix} \mathbf{L}\mathbf{q}_u \\ &+ \frac{1}{3}\mathbf{L}^{\mathrm{T}} \begin{bmatrix} \mathbf{N}_2^A(\mathbf{q}^A) & \mathbf{0} \\ \mathbf{0} & \mathbf{N}_2^B(\mathbf{q}^B) \end{bmatrix} \mathbf{L}\mathbf{q}_u = \mathbf{L}^{\mathrm{T}} \begin{Bmatrix} \mathbf{T}^{CC,A\mathbf{T}} \begin{Bmatrix} \mathbf{0} \\ \mathbf{f}(t)^A + \mathbf{r}(t)^A \end{Bmatrix} \\ \mathbf{T}^{CC,B\mathbf{T}} \begin{Bmatrix} \mathbf{0} \\ \mathbf{f}(t)^B + \mathbf{r}(t)^B \end{Bmatrix} \end{Bmatrix} \end{aligned} \tag{13}$$

The coupled equations are now in a functional form that can be used to predict the nonlinear dynamics of the assembly of geometrically nonlinear subcomponents. The implementation of this approach is relatively straightforward, and only requires subcomponent CC-NLROMs and the coupling matrix $\mathbf{L}$**;** no other numerical manipulation is necessary. The free or forced response to a given load/initial condition can be integrated using the reduced order equations in Eq. (13) at a significantly lower cost than integrating the full model of the assembly in physical coordinates. The substructuring methodology is demonstrated in the next section.

III. Numerical Results

The nonlinear substructuring approach with CC-NLROMs was applied to an example where two flat plates were coupled to one another along a continuous interface. The two geometrically nonlinear plates had simple supports at all the edges, and were modeled using the Abaqus® finite element package. A schematic of the case study is shown in Fig. 1, where the two substructures were coupled at all x, y, and z rotational DOF along the shared edge. The 9 inch by 9 inch plate was modeled with 1,296 (a 36×36 grid of) S4R shell elements, while the 9 inch by 6 inch plate had a total of 864 S4R shell elements. Each plate had a uniform thickness of 0.031 inches. The material properties were those of structural steel, where the Young's modulus was 29,700 ksi, shear modulus was 11,600 ksi, and mass density was $7.36*10^{-4}$ lb-s^2/in^4. Thin-walled plates such as these can experience large deformations even while the materials are within their elastic limit. A total of 37 nodes were along the connecting interface, which means there were 111 DOF describing the interface.

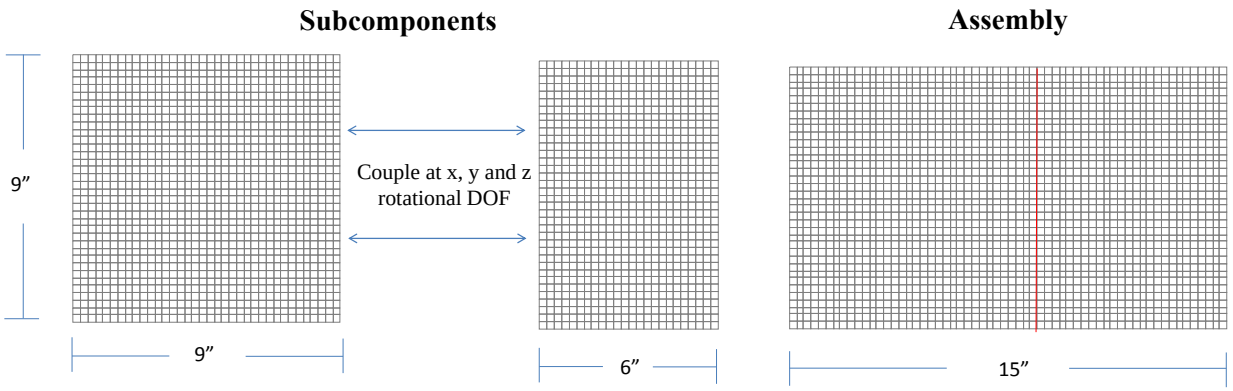

Figure 1. Coupling of two geometrically nonlinear plates with simple supports at all edges. The assembly FEA model had simple supports at all edges, and at each DOF along the red line where to two plate join.

A. Linear Substructuring Results

The linear mass and stiffness matrices of the plates were first used to determine how well this process works for the linear substructuring problem. The linear matrices were extracted from Abaqus® and reduced to the appropriate CB model with a truncated set of fixed-interface modes, and all 111 constraint modes. The linear natural frequencies of the fixed-interface modes are listed in Table 1. After assembling the traditional CB models, the characteristic constraint modes were computed, whose frequencies are given in the far right column of Table 1. The linear model with the truncated set of CC modes will be referred as the CC model. It was assumed that the target modes of the assembly were between 0 and 500 Hz, so the CC and CB models both included fixed-interface modes up to 1.5 times the frequency bandwidth. The 9 inch by 9 inch plate included the first 12 fixed-interface modes, and the 9 inch by 6 inch plate included the first 7 fixed-interface modes.

Table 1. Linear frequencies of the subcomponent modes used with the CC mode reduction.

Mode Number	Fixed-interface modes: 9”x9” plate	Fixed-interface modes: 9”x6” plate	Characteristic Constraint Modes
1	87.1 Hz	156.8 Hz	140.2 Hz
2	190.6 Hz	254.4 Hz	420.9 Hz
3	216.6 Hz	430.1 Hz	930.7 Hz
4	317.7 Hz	449.5 Hz	1660.5 Hz
5	371.4 Hz	547.0 Hz	2609.8 Hz
6	420.3 Hz	685.2 Hz	3785.1 Hz
7	494.6 Hz	717.4 Hz	5195.8 Hz
8	521.5 Hz	915.3 Hz	6852.9 Hz
9	630.0 Hz	965.6 Hz	8769.4 Hz
10	696.1 Hz	1013.8 Hz	10960.2 Hz
11	700.6 Hz	1021.3 Hz	13442.4 Hz
12	749.8 Hz	1182.7 Hz	16235.1 Hz
13	802.1 Hz	1295.0 Hz	19359.6 Hz
14	948.1 Hz	1426.6 Hz	22839.5 Hz
15	968.5 Hz	1441.5 Hz	26700.4 Hz
16	975.6 Hz	1567.4 Hz	30970.1 Hz

The characteristic constraint modes computed from the second modal analysis were used to further truncate the plate models by keeping only a few of the characteristic motions of the interface. The first three CC modes of the two plates are shown in Fig. 2. As seen by the deformation shapes, these modes capture the characteristic response of the interface caused the connection to the adjacent plate through the rotational DOF. The typical rule of thumb is to include modes up to 1.5 times the bandwidth of interest, but this is not well established for the use of CC modes.

The CC models here include the first 3 CC modes, which is not much beyond the bandwidth of interest, and were selected in order to capture the deformation at the interface.

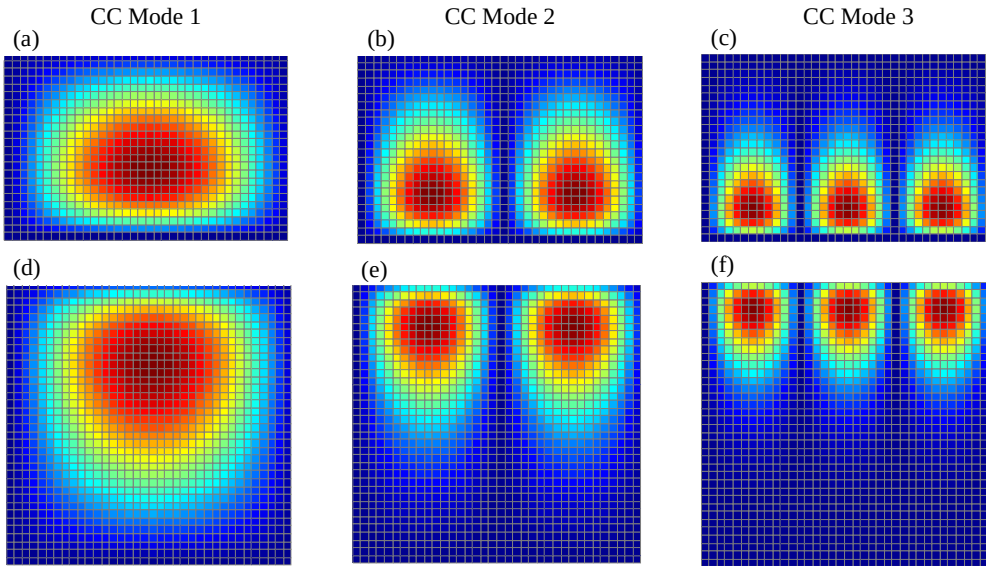

Figure 2. First three characteristic constraint modes of the (a-c) 9 inch by 6 inch plate and (e-f) 9 inch by 9 inch plate.

As a result, the CC model of the 9 inch by 9 inch plate included a total of 15 modes, while the 9 inch by 6 inch plate had only 10 modes. The assembly of these two models resulted in a set of linear equations with 22 DOF. The predicted natural frequencies resulting from the linear substructuring are presented in Table 2 and were compared with the modes computed from the full FEA model as a reference. The modes from the assembled CB models with all 111 interface DOF were also computed and shown in Table 2. The assembly of CB models had a total of 130 DOF, which was an order of magnitude larger than the assembly of CC models. When comparing the natural frequencies between 0 and 500 Hz, there is no discernible difference between predictions with the assemblies of CB models versus CC models, and both have frequency error of less than 0.4 % compared to the full order model. The reduction from 111 constraint modes in the CB models down to the 3 characteristic constrain modes in the CC models shows drastic reduction in order size without the loss of accuracy in the predicted modes of the assembly. In fact, the assembled models agree within 1.2% frequency error (with both approaches) up to the 19th mode, which has a frequency of 742.4 Hz. Beyond this frequency (which happens to be the cutoff frequency of the fixed-interface modes), the higher order modes (20, 21 and 22) cannot be trusted without adding more modes to the basis.

Table 2. Comparison of predicted natural frequencies for the assembled CB models and CC models.

Mode Number	Full FEA Assembly	CB models	% Error	CC models	% Error
1	78.4 Hz	78.4 Hz	0.00	78.4 Hz	0.00
2	135.1 Hz	135.1 Hz	-0.01	135.1 Hz	-0.01
3	185.7 Hz	185.7 Hz	0.00	185.7 Hz	0.00
4	203.0 Hz	203.0 Hz	-0.01	203.0 Hz	-0.01
5	239.5 Hz	239.5 Hz	-0.01	239.5 Hz	-0.01
6	306.4 Hz	306.4 Hz	-0.02	306.4 Hz	-0.02
7	365.7 Hz	366.3 Hz	-0.16	366.3 Hz	-0.16
8	368.2 Hz	368.3 Hz	-0.01	368.3 Hz	-0.01
9	419.7 Hz	419.8 Hz	-0.02	419.8 Hz	-0.02
10	434.1 Hz	434.2 Hz	-0.02	434.2 Hz	-0.02
11	474.4 Hz	476.3 Hz	-0.39	476.3 Hz	-0.39
12	485.5 Hz	485.6 Hz	-0.02	485.6 Hz	-0.02

The linear substructuring results agree very well with the full order model of the assembled plates. The accuracy of the predicted modes depends on the bandwidth of the fixed-interface modes, as well as the shapes and frequencies of the CC modes included in the reduction basis. In the next section, the CC-NLROMs were used to reduce the geometrically nonlinear plates in Fig. 1 and then were coupled to predict the behavior of the nonlinear assembly.

B. Nonlinear Substructuring Results

The CC-NLROMs of the two plate models were generated with the same set of fixed-interface and characteristic constraint modes as the linear case (12 fixed-interface with 3 CC modes for the 9 by 9 inch plate, and 7 fixed-interface with 3 CC modes for the 9 by 6 inch plate). The NLROM approach with all 111 constraint modes (known as the CB-NLROM approach in [9]) could not be used here, since the continuous interface has far too many connecting DOF and as a result, far too many basis vectors to generate the NLROM. For example, the 9 inch by 6 inch plate would have a total 118 basis vectors, and need 2,163,176 static load permutations to fit the 287,861 nonlinear stiffness coefficients for each mode in Eq. (10) [6]. In contrast, with only 3 CC modes, the 9 inch by 6 inch plate had a total 10 basis vectors, which required 1,160 static load permutations to fit the 275 nonlinear stiffness terms for each mode. In fact, it took about 5 hours to run the 4,080 static load cases that were needed to build the CC-NLROM for the 9 inch by 9 inch plate, and the 9 inch by 6 inch plate took 45 minutes, both on a desktop computer with 8 GB of RAM and an Intel® Core i7 CPU.

The CC-NLROMs were computed using the Implicit Condensation procedure in [10], where a series of forces were applied to the static equations of the FEA model in Eq. (1). The resulting displacements were extracted from Abaqus®, and a constrained fit [6] was used to determine the polynomial function in Eq. (10). When fitting the coefficients, the user must determine the magnitude of the applied force for each basis vector. In the authors' experience, choosing the correct force amplitude is not straightforward, and the best strategy seems to depend on the model of interest. Different force amplitudes can identify different coefficients in Eq. (10), and it can be difficult to determine which loads produce the best fit. The CC-NLROMs studied here were generated with three different amplitudes for the static loads. A constant displacement (CD) approach was used where the force amplitude f_i of the i^{th} mode (e.g. $\mathbf{F} = \mathbf{M}\phi_i f_i$) was chosen such that when applied to the linear structure, the force results in a maximum displacement on the order of some percentage of the thickness. To facilitate this discussion, the notation "CD [1]" will refer to a CC-NLROM generated with a constant displacement scaling strategy that scales each force to give a maximum linear displacement of 1 times the plate thickness (0.031 inches).

After choosing the basis vectors and the load scaling, the CC-NLROMs were generated and coupled, and the assembled equations of motion in Eq. (13) were used to compute the nonlinear normal modes (NNMs) [11] using the continuation algorithm in [12]. These branches of periodic solutions were compared, in Fig. 1, with those computed using the applied modal force (AMF) algorithm described in [13], which directly computes the NNMs of the full order FEA model of the plate assembly. The AMF algorithm is a non-intrusive approach which computes the NNMs directly from the finite element model within the native code at a significantly reduced cost, providing a reference solution to compare the results of the assembled CC-NLROMs. Recent studies suggest that if a reduced model accurately computes the NNMs of the full order model, then the model will also be able to accurately predict the response to various load environments [14]. The frequency-energy curves of the first 3 NNMs are plotted in Fig. 3 for CC-NLROMs generated with CD [1], CD [4] and CD [16].

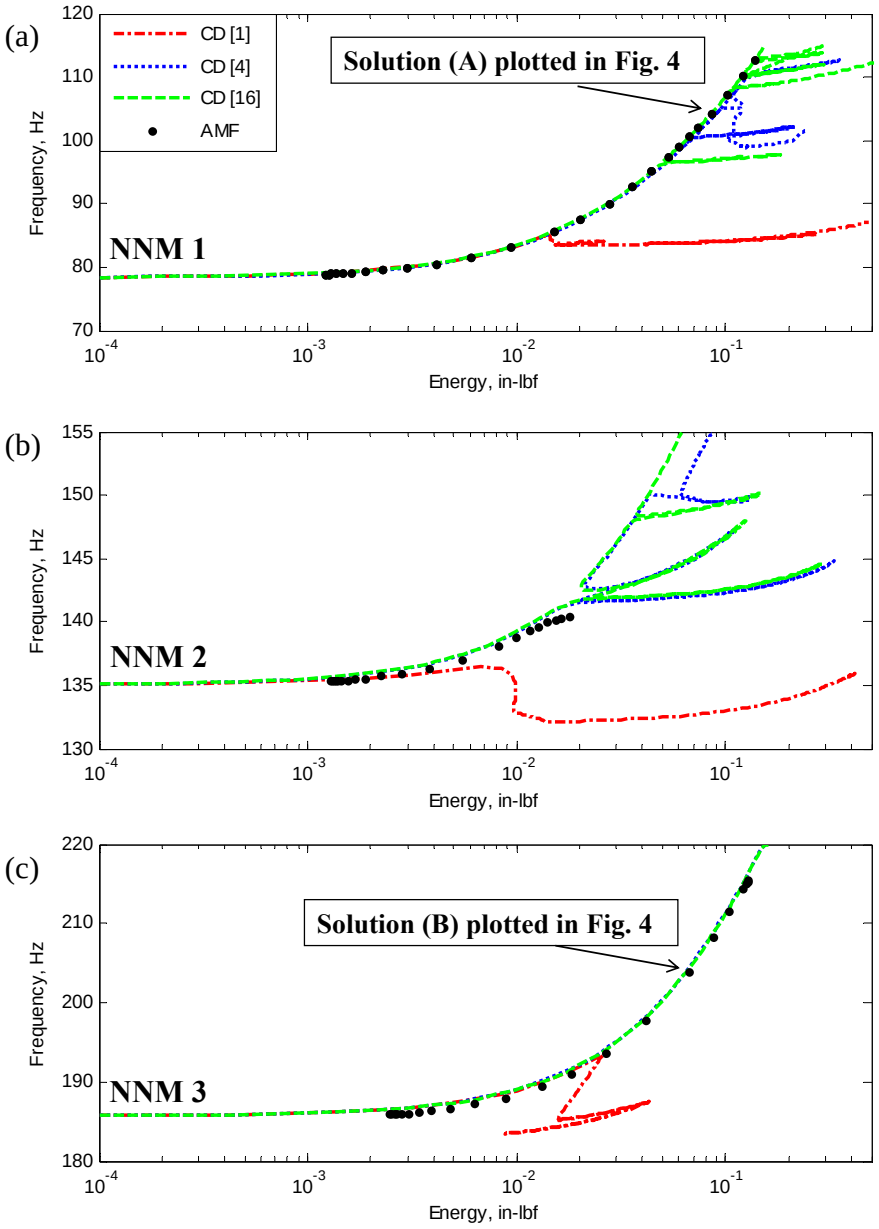

Figure 3. Frequency-energy curves for (a) NNM 1, (b) NNM 2 and (c) NNM 3 for the assembly in Fig. 1. The NNMs were computed from the (black dotted) full order model of the assembly, and the coupled CC-NLROMs with a CD load of (green dashed) 16x thickness, (blue short dashed) 4x thickness, and (red short dotted) 1x thickness.

The NNMs of the plate assembly showed hardening behavior, as indicated by the increase in fundamental frequency at higher energy periodic motions. This pure hardening behavior occurs with flat, geometrically nonlinear structures due to the stiffness increase caused by the membrane-bending coupling at high response amplitudes. Each NNM plotted in Fig. 3 started at a linear mode at low energy (or response amplitude), but as the response level increased, the motion began to exercise the geometric nonlinearity and the dynamics changed based on the state of the system. The computation of each curve with the AMF algorithm (black dotted) took on the order of days for a model with 12,861 DOF on the desktop computer mentioned earlier, so only a few "reference" solutions were available for comparison. All of the AMF solutions were along the main backbone, and further computation would be needed to capture the internal resonances (e.g. tongues emanating off the backbone). Each NNM from the CC-NLROM substructuring approach took about 10 minutes to compute. The excessive cost of the AMF algorithm on

the full order model reiterates the need to accurately reduce a detailed, nonlinear model down to a low order system of equations.

The NNMs computed with the CD [4] (blue short dashed) and CD [16] (green dashed) load scale factors were found to agree quite well with the frequency-energy curves computed from the full order model (black dotted). However, the NNMs from the CD [1] (red short dotted) model diverged from the others, indicating that this load level apparently did not exercise the nonlinearity enough to allow an adequate fit of the nonlinear stiffness coefficients. The NNM served as an excellent signature of the equations that can be used to quickly identify whether or not a model captures true physical behavior of the system. The CC-NLROMs with CD [1] showed a softening behavior after a slight hardening for each NNM. For the flat plates, the NNMs should stiffen with energy, so one would suspect that the CD [1] CC-NLROMs were inaccurate even if the AMF data were not available.

Both the CD [4] and CD [16] models agreed very well with one another along the backbone, and with the reference solutions from AMF. There was still some disagreement between the two ROMs at certain frequency/energy levels. The "tongues" sprouting from the backbones are known as internal resonances, and occur when 2 or more modes interact with one another. In fact, these modal interactions occur when the NNMs have commensurate frequencies at a fixed energy level (e.g. when a fractional frequency of a higher NNM matches the fundamental frequency of the NNM of interest). Along NNM 1, there were many internal resonances that show up with both models between 98 Hz and 112 Hz. It appeared that the relatively high modal density of the plate assembly offered a large number of mode interactions, making it difficult to fully assess the ability of the ROM to capture these using the continuation algorithm. However, since these mode interactions can be explained by the frequencies of all the NNMs along the backbone, the model should be able to accurately capture the internal resonances if all of the backbones have converged. The higher order NNMs should be checked for convergence as well, but this was not pursued in this work.

Figure 4 takes a closer look at periodic solutions marked (A) and (B) in Fig. 3. The time histories of the full order model, and the CD [4] and [16] CC-NLROM assemblies are plotted over one period. The predicted response in physical coordinates was projected onto the linear modes normalized to a maximum unit displacement. Hence, the relative amplitude of each modal coordinate corresponds to the maximum physical displacement amplitude for that mode. Solution (A) occured along the backbone of NNM 1 around a frequency of 104.3 Hz. The time histories in the left column of Fig. 4 show that the response was dominated by the first bending mode, but has some contribution of higher order bending modes as well (the legend orders the modes based on the largest value over the period). All of the models predicted that the next highest contributor to the response would be the 2nd mode. It is interesting to note that the AMF and CD [16] CC-NLROM agree in terms of the order in which the five dominant modes appear with the amplitude of the modal coordinates, but the CD [4] model has different modes contributing (e.g. modes 4 and 21). While these amplitudes were small compared to the dominant motion of mode 1, the fact that mode 21 becomes active was a bit concerning since this linear mode was too high in frequency to be computed accurately by linear substructuring (in fact, there was a 64% frequency error for the prediction of the 21st mode).

Solution (B) in the right column of Fig. 4 shows the periodic motion of NNM 3 at a frequency of 203.9 Hz. Again, all three models show the motion was dominated by the 3rd bending mode. Each of the CC-NLROM assemblies agree with AMF that the next highest contributing mode was mode 5, but the other contributors do not agree with the full order model. The assembled CC-NLROMs show a motion with significant contribution from the 20th bending mode. Again, this mode was not accurately predicted by the linear substructuring case either (frequency error of 79%), and probably cannot be trusted if it introduced itself into the periodic response. In fact, looking at NNM 3 in Fig. 3, the backbone appeared to have some slight disagreement with the AMF results, so this could probably be explained by the fact that the CC-NLROM assemblies did not have enough modes in basis to capture the periodic solutions along NNM 3. More modes could be added to remedy this situation, but this was not explored in this paper.

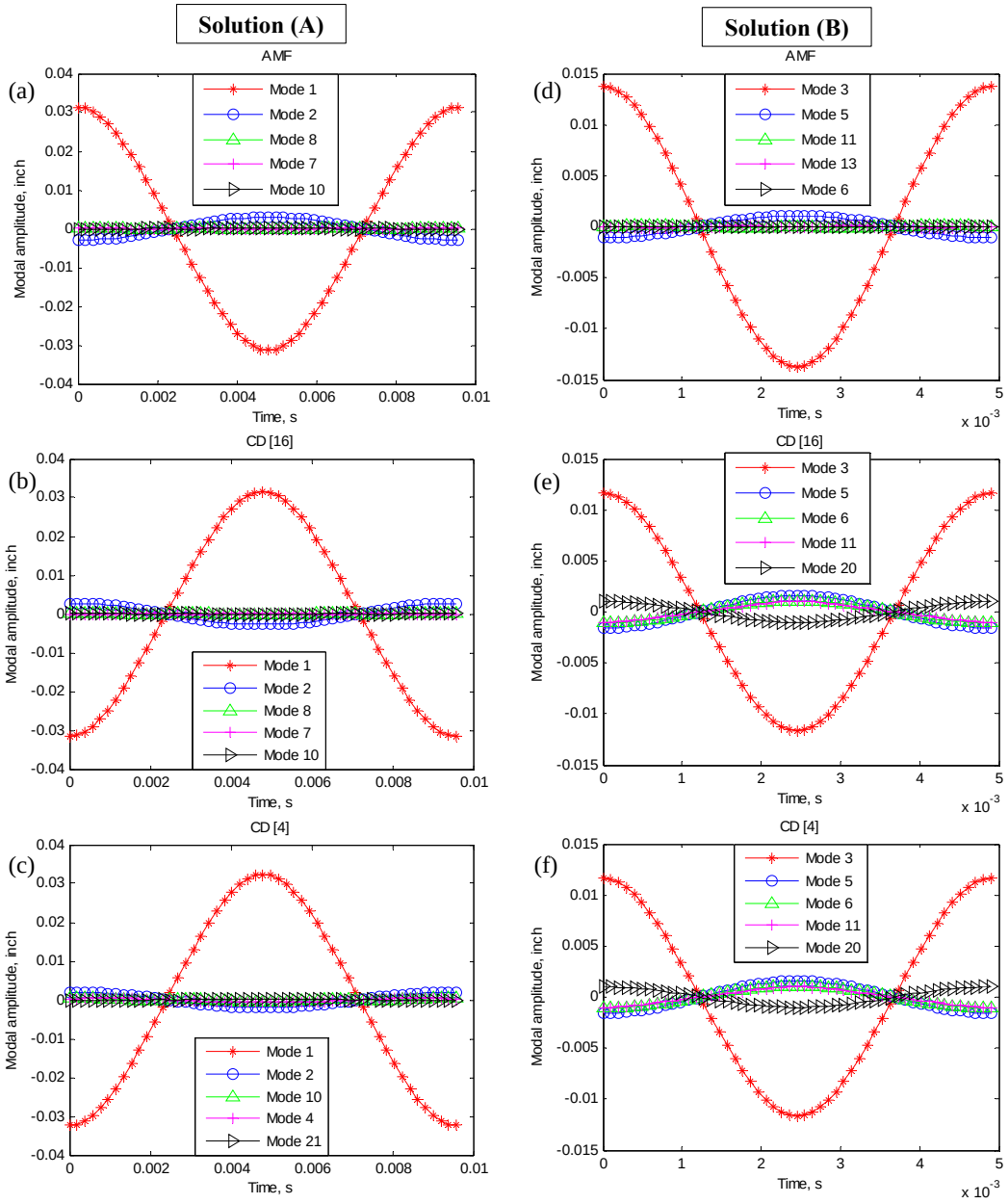

Figure 4. Comparison of time histories from solution (A) and (B) in Fig. 3 computed from the (a,d) full order model using the AMF algorithm, (b,e) CD [16] CC-NLROM and (c,f) CD [4] CC-NLROM. The coordinates are projections of the periodic response onto the linear modes normalized to a maximum unit displacement.

IV. Conclusion

This paper presented an approach to generate nonlinear reduced order models of a geometrically nonlinear subcomponent using fixed-interface modes and characteristic constraint modes [3], and used these models with substructuring in order to approximate the behavior of large scale assemblies of nonlinear finite element models. The characteristic constraint modes allowed the number of modes in the reduced space to be drastically truncated, lowering the computational cost to identify the nonlinear stiffness coefficients in the nonlinear modal equations. By assembling the NLROMs, the equations of motion of the assembly are orders of magnitude smaller than the full order finite element model, hence speeding up the computational time to perform detailed structural analysis. A substructuring approach has the advantage of breaking the complicated structure into several smaller, more manageable subcomponents, and then using these FEA models to predict the dynamics of a global assembly (e.g. exterior structure of an aircraft).

The new CC-NLROM approach was demonstrated by coupling two thin plates with geometric nonlinearity. The NNMs were computed from the assembled CC-NLROMs generated with three different load levels. The resulting frequency-energy curves provided a good metric to compare the results with a known reference solution from the full order model. It was found that the CC-NLROMs generated with the CD [1] scaling level offered very poor results as indicated by the first 3 NNMs. Even without a reference solution, engineering judgment could be used to justify that it was a poor model. The CD [4] and CD [16] models showed excellent agreement between each other, and with the full order model along the backbone. An investigation into the time histories of two select periodic motions along the curves showed that CC-NLROM models were quite accurate for NNM 1, but could have some error in NNM 3. A hypothetical next step in this analysis would be to check the convergence of the scaling factors by comparing a CD [32] model, and also adding more modes to the basis set. As more modes are added, it is suspected that the NNMs of the assembly would converge to those of the full order model.

Future work will further explore the issue with the load scaling factors, as well as the use of the expansion in [10] with the new basis vectors. The expansion allows for the "expansion" of membrane displacements from the bending motions of the ROM in order to more accurately predict the physical deformations (and ultimately stresses) caused by the vibrations. The nonlinear substructuring approach will be attempted on a high fidelity model where the reference data from AMF will not be available due to excessive computational cost (as will likely be the case in most of the applications of interest). The nonlinear normal modes will serve as a metric to perform a convergence study, where modes are added to the basis set of the reduced subcomponents and the NNMs of the assembly should begin to converge towards the true NNMs of the full order model.

Acknowledgments

This work was supported by the Air Force Office of Scientific Research, Award # FA9550-11-1-0035, under the Multi-Scale Structural Mechanics and Prognosis program managed by Dr. David Stargel. The authors also wish to thank Dr. Joseph Hollkamp and other collaborators in the Structural Sciences Center at the Air Force Research Laboratory for providing the Abaqus® interface that was used as well as for many helpful suggestions and discussions. The authors were also partially supported by Sandia National Laboratories under Contract No. DE-AC04-94AL85000 with the U.S. Department of Energy.

References

[1] W. C. Hurty, "Dynamic analysis of structural systems using component modes," *AIAA Journal*, vol. 3, pp. 678-685, 1965/04/01 1965.

[2] R. R. J. Craig and M. C. C. Bampton, "Coupling of Substructures for Dynamic Analysis," *AIAA Journal*, vol. 6, pp. 1313-1319, 1968.

[3] M. P. Castanier, Y. Tan, and C. Pierre, "Characteristic Constraint Modes for Component Mode Synthesis," *AIAA Journal*, vol. 39, pp. 1182-1187, 2001.

[4] J. J. Hollkamp, R. W. Gordon, and S. M. Spottswood, "Nonlinear modal models for sonic fatigue response prediction: a comparison of methods," *Journal of Sound and Vibration*, vol. 284, pp. 1145-63, 2005.

[5] M. P. Mignolet, A. Przekop, S. A. Rizzi, and S. M. Spottswood, "A review of indirect/non-intrusive reduced order modeling of nonlinear geometric structures," *Journal of Sound and Vibration*, vol. 332, pp. 2437-2460, 2013.

[6] R. W. Gordon and J. J. Hollkamp, "Reduced-Order Models for Acoustic Response Prediction," Air Force Research Laboratory (AFRL), Wright-Patterson Air Force Base, OH AFRL-RB-WP-TR-2011-3040, 2011.

[7] R. Perez, X. Q. Wang, A. Matney, and M. P. Mignolet, "Reduced Order Model For the Geometric Nonlinear Response of Complex Structures," presented at the ASME 2012 International Design Engineering Technical Conferences IDETC/CIE, Chicago, Illinois, 2012.

[8] R. J. Kuether and M. S. Allen, "Nonlinear Modal Substructuring of Systems with Geometric Nonlinearities," in *54th AIAA/ASME/ASCE/AHS/ASC Structures, Structural Dynamics, and Materials Conference*, Boston, Massachusetts, 2013.

[9] R. J. Kuether and M. S. Allen, "Craig-Bamptom Substructuring for Geometrically Nonlinear Subcomponents," presented at the 32nd International Modal Analysis Conference (IMAC XXXII), Orlando, Florida, 2014.

[10] J. J. Hollkamp and R. W. Gordon, "Reduced-order models for nonlinear response prediction: Implicit condensation and expansion," *Journal of Sound and Vibration*, vol. 318, pp. 1139-1153, 2008.

[11] G. Kerschen, M. Peeters, J. C. Golinval, and A. F. Vakakis, "Nonlinear normal modes. Part I. A useful framework for the structural dynamicist," *Mechanical Systems and Signal Processing*, vol. 23, pp. 170-94, 2009.
[12] M. Peeters, R. Viguié, G. Sérandour, G. Kerschen, and J. C. Golinval, "Nonlinear normal modes, Part II: Toward a practical computation using numerical continuation techniques," *Mechanical Systems and Signal Processing*, vol. 23, pp. 195-216, 2009.
[13] R. J. Kuether and M. S. Allen, "A Numerical Approach to Directly Compute Nonlinear Normal Modes of Geometrically Nonlinear Finite Element Models," *Mechanical Systems and Signal Processing*, 2013 (submitted).
[14] R. J. Kuether, M. R. Brake, and M. S. Allen, "Evaluating Convergence of Reduced Order Models Using Nonlinear Normal Modes," presented at the 32nd International Modal Analysis Conference (IMAC XXXII), Orlando, Florida, 2014.